Acta Cryst. (1999). B**55**, 8–16

Temperature-dependent neutron powder diffraction evidence for splitting of the cationic sites in ferroelectric $PbHf_{0.4}Ti_{0.6}O_3$

C. Muller,[a]* J.-L. Baudour,[a] V. Madigou,[a] F. Bouree,[b] J.-M. Kiat,[b,c] C. Favotto[d] and M. Roubin[d]

[a]*Laboratoire des Matériaux Multiphasés et Interfaces, Université de Toulon et du Var, BP 132, 83957 La Garde CEDEX, France,* [b]*Laboratoire Léon Brillouin, CE-Saclay, 91191 Gif-sur-Yvette, France,* [c]*Laboratoire de Chimie Physique du Solide, URA CNRS 453, Ecole Centrale de Paris, 92295 Châtenay-Malabry CEDEX, France, and* [d]*Laboratoire des Matériaux à Finalités Spécifiques, Université de Toulon et du Var, BP 132, 83957 La Garde CEDEX, France. E-mail: muller@univ-tln.fr*

(*Received 29 January 1998; accepted 20 April 1998*)

Abstract

Temperature-dependent neutron powder diffraction experiments (diffractometer 3T2-LLB, Saclay, France, λ = 1.227 Å) have been performed on the perovskite-like lead hafnate titanate $PbHf_{0.4}Ti_{0.6}O_3$. This compound belongs to the solid solution denoted PHT, which derives from the well known ferroelectric PZT series. It exhibits a ferroelectric-to-paraelectric phase transition around 620 K, between the low-temperature tetragonal phase and the high-temperature cubic phase. The tetragonal structure of the ferroelectric phase has been refined at 10 and 300 K using a Rietveld-type method: space group $P4mm$ with $Z = 1$; a_t = 3.999 (1), c_t = 4.120 (1) Å, c/a = 1.030, V = 65.89 Å^3 at 10 K; a_t = 4.012 (1) and c_t = 4.100 (1) Å, c/a = 1.022, V = 65.99 Å^3 at 300 K. The cubic structure of the paraelectric phase has also been refined at 720 K: space group $Pm\bar{3}m$, $Z = 1$, a_c = 4.046 (1) Å, V = 66.23 Å^3. Cation displacements and oxygen-octahedra elongations have been observed as a function of temperature. Evidence for peculiar behaviour associated with the relative shifts of the Hf and Ti atoms (thought until now to be on the same crystallographic site) was found through an anomaly of the mean-square atomic displacements of the Hf/Ti pseudo-nucleus. The PDF Nos for $PbHf_{0.4}Ti_{0.6}O_3$ are 48-49-9 and 48-49-10.

1. Introduction

In the field of dielectric ceramics the lead zirconate titanate $PbZr_xTi_{1-x}O_3$ (PZT) solid solution is of great technological interest, especially in electromechanical transducer applications (Jaffe *et al.*, 1955). The complete substitution of Zr^{4+} cations by Hf^{4+} ions leads to a new isomorphic series formulated as $PbHf_xTi_{1-x}O_3$ (PHT), which also exhibits strong ferroelectric properties. Although the phase diagram of the PHT family has been much less studied than PZT, the rhombohedral Hf-rich phase is also separated from the tetragonal Ti-rich phase by a diffuse morphotropic phase boundary (MPB; Jaffe *et al.*, 1955). In this region, for which x is close to 0.5, the coexistence of the rhombohedral and tetragonal phases enhances the dielectric and mechanical properties (Favotto, 1997; Favotto *et al.*, 1998). In the PZT series for compositions with x greater than 0.9 the symmetry is orthorhombic (Glazer & Mabud, 1978).

The crystallographic structures and the electrical properties of the extreme binary compounds $PbTiO_3$ ($x = 0$) and $PbHfO_3$ ($x = 1$) are well known. At room temperature the ferroelectric $PbTiO_3$ crystallizes in a tetragonal structure with space group $P4mm$ (No. 99), $Z = 1$ and $c/a \simeq 1.064$ (Shirane & Pepinsky, 1956; Glazer & Mabud, 1978). Fixing the Pb atom at the origin on site 1a at (0, 0, 0), the positions of the other atoms in the unit cell are: Ti on site 1b at ($\frac{1}{2}$, $\frac{1}{2}$, $\frac{1}{2} + \delta z_{Ti}$), O1 on site 1$b$ at ($\frac{1}{2}$, $\frac{1}{2}$, δz_{O1}) and O2 on site 2c at ($\frac{1}{2}$, 0, $\frac{1}{2} + \delta z_{O2}$). The ferroelectricity is due to correlative displacement in the same direction of the Pb^{2+} and Ti^{4+} cations with respect to the oxygen octahedra. The shifts occurring along the c axis are $\sim$0.48 Å for Pb and 0.32 Å for Ti (Glazer & Mabud, 1978).

On the other hand, $PbHfO_3$ is antiferroelectric and at room temperature has orthorhombic symmetry with space group $Pbam$ (No. 55), $Z = 8$ (Shirane & Pepinsky, 1953; Jankowska-Sumara *et al.*, 1995; Corker *et al.*, 1998). Its structure, an isotype of that of $PbZrO_3$ (Jona *et al.*, 1957; Glazer *et al.*, 1993; Corker *et al.*, 1997), can be viewed as a superstructure of the tetragonal perovskite-like structure with $c/a \simeq 0.989$ (Corker *et al.*, 1998; Madigou *et al.*, 1998). The orthorhombic cell parameters (a_o, b_o and c_o) are linked to the tetragonal ones (a_t, b_t and c_t) according to the relations

$$a_o = a_t(2^{1/2}),\ b_o = 2a_t(2^{1/2}),\ c_o = 2c_t.$$

With respect to the oxygen octahedron, the Pb and Hf atoms are shifted by 0.24 and 0.17 Å, respectively, along the [100] direction of the orthorhombic cell.

Above the Curie temperature T_C, which decreases along with x (760 K for $PbTiO_3$ to 490 K for $PbHfO_3$), all the compounds crystallize in a paraelectric cubic perovskite-type structure described in the space group

© 1999 International Union of Crystallography
Printed in Great Britain – all rights reserved

$Pm\bar{3}m$ (No. 221), the z shifts δz of the oxygen ions and cations being equal to zero.

The aim of this paper is the study of an intermediate composition between $PbTiO_3$ and $PbHfO_3$, *i.e.* a composition close to $PbHf_{0.5}Ti_{0.5}O_3$. We report here the results obtained from neutron powder diffraction data collected on the compound $PbHf_{0.4}Ti_{0.6}O_3$ at the following temperatures: 10 and 300 K for the tetragonal phase, and 720 K for the cubic phase ($T_C \simeq 620$ K). Neutron diffraction is a better technique than X-ray diffraction for providing reliable oxygen-atom positions and atomic displacement parameters.

Particular attention has been turned towards the temperature dependence of the Pb and Hf/Ti atomic shifts and the elongation of the oxygen octahedra. Through the isotropic or anisotropic mean-square atomic displacements, the relative displacement of the Hf and Ti nuclei is discussed below and above the Curie temperature. Furthermore, an unusually large value of the atomic displacement parameter of Pb observed above T_C has been interpreted.

2. Experimental

2.1. *Sample synthesis*

The sol–gel process has been used to produce ceramic PHT materials at significantly lower temperatures than the traditional ceramic fabrication method. The process is basically a wet chemical technique consisting of the following steps (Favotto *et al.*, 1996): (i) preparation of the appropriate metal alkoxide solution [hafnium(IV) isopropoxide, titanium(IV) isopropoxide and lead(II) acetate], (ii) polymerization, (iii) gel drying (333 K) and (iv) firing (1023 K).

The chemical composition was checked by energy-dispersive spectroscopy (EDS) using a transmission electron microscope. The K factors of the Ti K and Hf L peaks were successively calibrated using samples of $PbTiO_3$ and $PbHfO_3$. Analyses of several particles led to an Hf chemical composition of 0.40 ± 0.02.

2.2. *Data collection*

Neutron powder diffraction experiments were performed on the high-resolution diffractometer 3T2 at the Orphée reactor at the Laboratoire Léon Brillouin (Saclay, France) with an incident neutron wavelength of 1.227 Å. The powdered sample was contained in a vanadium can and the resulting cell was placed either in an He gas-flow cryostat (data collected at 10 K) or in a furnace (data collected at 720 K). Data were also collected at room temperature. The intensities were measured by a bank of 20 ^{3}He counters. Full experimental details are given in Table 1.

2.3. *Structure refinements*

The neutron powder diffraction profiles were fitted using a Rietveld-type method implemented in the program *Fullprof* (Rodriguez-Carvajal, 1990).† The observed profiles were described using a pseudo-Voigt profile shape function ($\eta \simeq 0.4$) and the instrumental broadening respected the classical Caglioti function $(U \tan^2\theta + V \tan\theta + W)^{1/2}$, where U, V and W are refinable parameters (Caglioti *et al.*, 1958). The background was adjusted using a polynomial function. Systematic error corrections for zero-point and asymmetry were applied. The coherent scattering lengths used in the refinement were: $b_{Pb} = 0.940 \times 10^{-12}$, $b_{Hf} = 0.780 \times 10^{-12}$, $b_{Ti} = -0.344 \times 10^{-12}$ and $b_O = 0.580 \times 10^{-12}$ cm. For the composition corresponding to the formula $PbHf_{0.4}Ti_{0.6}O_3$ the scattering length of the pseudo-nucleus Hf/Ti is 0.106×10^{-12} cm.

For the ferroelectric tetragonal phase (at 10 and 300 K), the starting crystallographic model corresponds to the $PbTiO_3$ structure. The atomic positions are given in the non-centrosymmetric space group $P4mm$. Taking Pb at the origin, the positions of the Hf/Ti and O atoms are described in terms of three parameters $z_{Hf/Ti} = \frac{1}{2} + \delta z_{Hf/Ti}$, $z_{O1} = \delta z_{O1}$ and $z_{O2} = \frac{1}{2} + \delta z_{O2}$ representing the atomic shifts from ideal perovskite positions along the ferroelectric axis, *i.e.* the c axis. The pseudo-centre of the oxygen octahedron was assumed to be randomly shared by Hf and Ti nuclei in agreement with the composition ratio x. For each atom either isotropic or anisotropic mean-square atomic displacements were also refined.

For the high-temperature cubic phase ($T = 720$ K) the atomic positions were described in the $Pm\bar{3}m$ space group with reference to the perovskite structure.

3. Structure refinements with Hf and Ti nuclei on the same crystallographic site

3.1. *Ferroelectric tetragonal structure*

Neutron diffraction profiles collected at 10 and 300 K were fitted starting from the tetragonal structural model of $PbTiO_3$ (Glazer & Mabud, 1978). Different starting models were also tried and all of them gave the same outcome. After preliminary refinement to establish the scale factor and the instrumental parameters, several cycles were carried out refining atomic positions, an isotropic overall atomic displacement parameter B_{over} and the Hf/Ti occupancy. Then an isotropic atomic displacement parameter B_{iso} was independently refined for Pb, Hf/Ti and O nuclei. Final coordinates, Hf/Ti occupancy and displacement parameters B_{iso} are given in Table 2. Observed, calculated and difference neutron diffraction profiles at 10 and 300 K are given in Figs. 1(*a*)

† Supplementary data for this paper are available from the IUCr electronic archives (Reference: SH0116). Services for accessing these data are described at the back of the journal.

Table 1. *Details of the temperature-dependent neutron powder diffraction experiments*

	10 K	300 K	720 K
Crystal data			
Chemical formula	$PbHf_{0.4}Ti_{0.6}O_3$	$PbHf_{0.4}Ti_{0.6}O_3$	$PbHf_{0.4}Ti_{0.6}O_3$
Chemical formula weight	355.33	355.33	355.33
Cell setting	Tetragonal	Tetragonal	Cubic
Space group	*P*4*mm*	*P*4*mm*	$Pm\bar{3}m$
a (Å)	3.999 (1)	4.012 (1)	4.046 (1)
c (Å)	4.120 (1)	4.100 (1)	
V (Å^3)	65.89	65.99	66.23
Z	1	1	1
μr	0.08	0.08	0.08
Data collection			
Radiation type	Neutron	Neutron	Neutron
Diffractometer	3T2, LLB-Saclay	3T2, LLB-Saclay	3T2, LLB-Saclay
Wavelength (Å)	1.227	1.227	1.227
Sample container	Vanadium can	Vanadium can	Vanadium can
2θ range (°)	6–125.7	6–120.55	6–125.7
2θ step (°)	0.05	0.05	0.05
Monochromator	Ge (335)	Ge (335)	Ge (335)
Instrumental geometry	20 ^{3}He detectors	20 ^{3}He detectors	20 ^{3}He detectors
Sample environment	Cryostat	None	Furnace
Refinement			
Background	Polynomial function	Polynomial function	Polynomial function
Excluded regions (°)	6–15; 109–125.7	6–15; 109–120.55	6–23; 109–125.7
Full width at half maximum	Caglioti function	Caglioti function	Caglioti function
Profile shape function	Pseudo-Voigt	Pseudo-Voigt	Pseudo-Voigt
No. of reflections	69	69	29
No. of parameters refined	20	20	13
Weighting scheme	$w = 1/\sigma^2$; $\sigma^2 = y_i$	$w = 1/\sigma^2$; $\sigma^2 = y_i$	$w = 1/\sigma^2$; $\sigma^2 = y_i$
R_p	0.087	0.073	0.046
R_{wp}	0.110	0.095	0.057
R_{exp}	0.057	0.047	0.055
χ^2	3.73	4.05	1.05
Computer programs			
Structure refinement	*Fullprof* (Rodriguez-Carvajal, 1990)	*Fullprof* (Rodriguez-Carvajal, 1990)	*Fullprof* (Rodriguez-Carvajal, 1990)
Structure graphics	*CaRIne* (Monceau & Boudias, 1996)	*CaRIne* (Monceau & Boudias, 1996)	*CaRIne* (Monceau & Boudias, 1996)

$R_p = 100 \times \sum_i |y_i - y_{ci}| / \sum_i y_i$; $R_{wp} = 100 \times [\sum_i w_i (y_i - y_{ci})^2 / \sum_i w_i y_i^2]^{1/2}$.

and 1(*b*), respectively. The difference profiles reveal that while the single lines are symmetrical, the double lines show a peculiar profile with a supplementary diffracted intensity between the lines. This intensity can be associated with an additional phase, which is probably a paraelectric cubic phase whose Bragg reflections are in the same angular domain as those of the tetragonal phase. The broadened lines of this additional phase were fitted using a cell-constrained refinement only, the intensity being a free variable (pattern matching mode). The corresponding cell parameter was 4.032 (1) Å at 10 K. The chosen profile shape function was Gaussian and the parameters U, V and W of the Caglioti function were independent of those of the tetragonal phase. The inclusion of this phase in the refinement gives a better fit between the observed and calculated profiles (R_p = 0.061, R_{wp} = 0.078, R_{exp} = 0.057 and χ^2 = 1.88), particularly between the double lines (Fig. 2), and does not modify the structural results discussed hereafter. This additional phase, probably present as small particles (< 100 Å), disappears when the compound is fired at high temperature (T > 1300 K). Studies are under way. A similar phenomenon, which may also be related to the ferroelectric domain walls, has already been studied in the $BaTiO_3$ perovskite-type structure (Takeuchi *et al.*, 1995; Valot *et al.*, 1996; Floquet *et al.*, 1997) and in the PZT series (Li *et al.*, 1993).

The refined cell parameters (Table 1) are similar to those referred to earlier (Jaffe *et al.*, 1955) and the optimized Hf/Ti occupancy x = 0.42 (1) is very close to 0.40, the expected value. This composition, also obtained from X-ray powder diffraction data, is in agreement with the EDS analysis (x = 0.40 ± 0.02).

The refinements exhibit an anomaly on the Hf/Ti site in the negative value of the atomic displacement parameter B_{iso} [Hf/Ti]. This unphysical value cannot be attributed to systematic errors such as sample absorption. For Debye–Scherrer geometry, the program *Full-*

prof (Rodriguez-Carvajal, 1990) corrects the intensities for the effects of sample absorption. All the structure refinements reported in this paper were performed applying this correction, but the sample absorption being small ($\mu r = 0.08$), this correction does not improve the R factors and does not modify the values of the atomic displacement parameters.

When anisotropic atomic displacement parameters are introduced (Table 3), the R factors are improved (R_F = 0.049 at 10 K and 0.043 at 300 K) and the refinement leads to a high negative value of the B^{33} parameter associated with the Hf/Ti pseudo-nucleus, the atomic coordinates remaining unchanged. In all cases the standard uncertainties (s.u.'s) are always considerably smaller than the value of the refined parameter: ~40% for B_{iso} and B^{33}. Therefore, the negative value of B_{iso} and the strong anisotropy of the displacement ellipsoid along z observed through the B^{33} parameter can be correlated with an anomaly of the Hf/Ti displacements along the c axis. This question is discussed and a plausible explanation is proposed in §4.

From the refinement the cation z shifts δz (Table 2) and interatomic distances have been calculated. At 10 and 300 K the Pb and Hf/Ti nuclei move in the same direction ($\delta z > 0$) with respect to the oxygen octahedron. This is consistent with the ferroelectric behaviour observed below the Curie temperature in the PHT solid solution. The Pb displacement (0.45 Å at 10 K and 0.39 Å at 300 K) is similar to that obtained in $PbTiO_3$ (0.48 Å at 300 K; Glazer & Mabud, 1978). Moreover, the pseudo-atom Hf/Ti seems to be closer to the centre of the oxygen octahedron than Ti in $PbTiO_3$ (0.09 Å rather than 0.32 Å at 300 K). The large shift of the Pb atom along the ferroelectric axis brings an appreciable change in the bonds between Pb and O atoms. At 300 K the Pb—O distances vary in the range 2.86–3.16 Å. The environment of Pb in $PbHf_{0.4}Ti_{0.6}O_3$ is quite similar to that in $PbTiO_3$. The relatively low spread of the distances Hf/Ti—O (2.01–2.08 Å at 300 K) shows that the pseudo-atom Hf/Ti is close to the centre of the oxygen octahedron. However, the marked difference at room temperature between the distances O2—O1*a* (2.92 Å) and O2—O1*b* (2.82 Å) compared to 2.86 and 2.84 Å, respectively, in $PbTiO_3$ (Table 5) shows clearly that in the $PbHf_{0.4}Ti_{0.6}O_3$ structure the oxygen octahedron is more distorted along the c axis than in $PbTiO_3$.

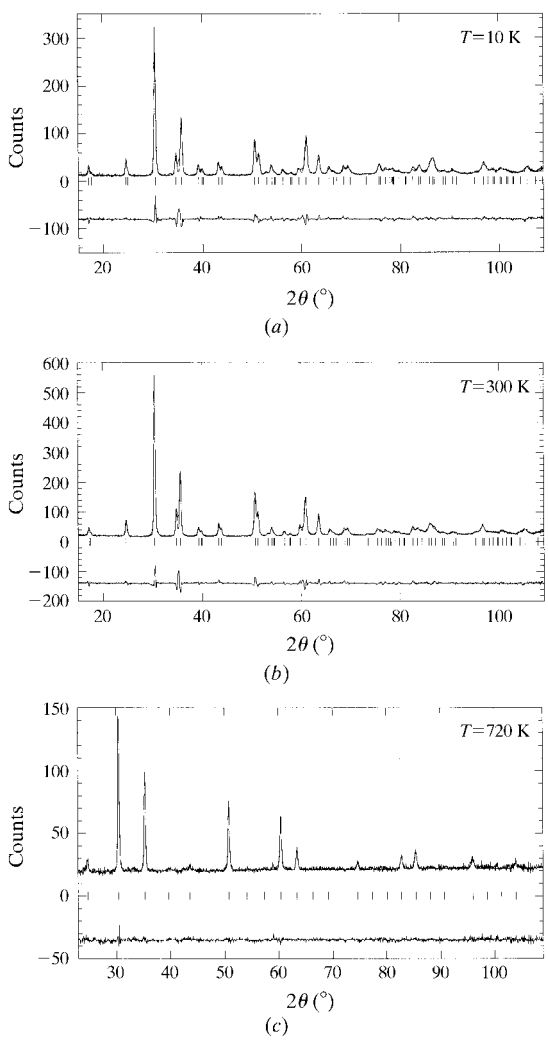

Fig. 1. Observed and calculated neutron diffraction profiles and their difference curves for $PbHf_{0.4}Ti_{0.6}O_3$ at (*a*) 10, (*b*) 300 and (*c*) 720 K.

3.2. *Paraelectric cubic structure*

The paraelectric cubic structure has been refined at 720 K. The atomic coordinates and isotropic atomic displacement parameters are given in Table 2. Fig. 1(*c*) shows the calculated and observed profiles for the cubic phase.

The non-distorted rigid-octahedron model corresponding to the cubic structure gives good results with reasonable R factors (Table 2). As for the tetragonal structure refinement, the refined occupancy x is 0.42. The most noticeable feature is the unusually small positive value of the parameter B_{iso} [Hf/Ti] associated with the Hf/Ti vibrations at this temperature (0.3 $Å^2$ at 720 K). Therefore, the anomaly of the mean-square

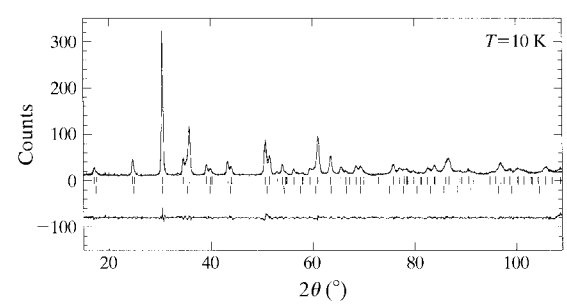

Fig. 2. Full profile adjustment including an additional cubic phase in the refinement of the tetragonal structure (data collected at 10 K).

Table 2. *Fractional atomic coordinates, Hf/Ti occupancy and isotropic atomic displacement parameters B_{iso} from the neutron Rietveld refinement of $PbHf_{0.4}Ti_{0.6}O_3$*

Cation shifts δz are given with respect to the centre of the oxygen octahedron.

	$PbTiO_3$, 300 K (Glazer & Mabud, 1978)	$PbHf_{0.4}Ti_{0.6}O_3$, 10 K	$PbHf_{0.4}Ti_{0.6}O_3$, 300 K	$PbHf_{0.4}Ti_{0.6}O_3$, 720 K
z_{Ti}	0.539 (2)	—	—	—
$z_{Hf/Ti}$	—	0.579 (4)	0.573 (3)	1/2
z_{O1}	0.114 (2)	0.096 (2)	0.082 (2)	0
z_{O2}	0.617 (2)	0.617 (2)	0.601 (2)	1/2
B_{iso} [Pb] (Å^2)	0.69 (9)	0.70 (11)	1.49 (12)	4.06 (28)
B_{iso} [Ti] (Å^2)	0.03 (17)	—	—	—
B_{iso} [Hf/Ti] (Å^2)	—	−0.58 (26)	−0.37 (23)	0.33 (42)
B_{iso} [O1] = B_{iso} [O2] (Å^2)	0.44 (6)	0.82 (8)	1.29 (7)	2.57 (12)
Hf chemical occupancy	—	0.42 (1)	0.42 (1)	0.42 (1)
R_{Bragg}	—	0.0682	0.0592	0.0262
R_F	—	0.0552	0.0530	0.0653
δz_{Pb} (Å)	0.482 (3)	0.453 (3)	0.388 (3)	0
δz_{Ti} (Å)	0.32 (1)	—	—	0
$\delta z_{Hf/Ti}$ (Å)	—	0.13 (2)	0.09 (1)	0

$R_{Bragg} = 100 \times \sum_k |I_k - I_k^{calc}| / \sum_k I_k$; $R_F = 100 \times \sum_k |(I_k)^{1/2} - (I_k^{calc})^{1/2}| / \sum_k (I_k)^{1/2}$.

Hf/Ti displacements, which are much lower than the others, persists even in the paraelectric phase.

It is also surprising that the value of the B_{iso} [Pb] parameter (4.1 Å^2) is significantly higher than the others, the Pb ions being the heaviest atoms in the structure. Such a phenomenon has already been observed in the relaxor ferroelectric perovskite $PbSc_{1/2}Nb_{1/2}O_3$ by Malibert *et al.* (1997), in $PbHfO_3$ by Kwapulinski *et al.* (1994), in $PbTiO_3$ by Nelmes *et al.* (1990) and in $PbZr_{0.9}Ti_{0.1}O_3$ by Glazer *et al.* (1978). A possible explanation is a static or dynamic disorder in the Pb sublattice. The Pb ions would be randomly displaced, occupying one of the 12 equivalent (x, x, 0) positions instead of the (0, 0, 0) position (Kwapulinski *et al.*, 1994; Malibert *et al.*, 1997).

Table 3. *Anisotropic atomic displacement parameters B^{ij} (Å^2)*

For anisotropic atomic displacements, the exponent term takes the form

$$T = \exp[(-\tfrac{1}{4})(B^{11}h^2a^{*2} + B^{22}k^2b^{*2} + B^{33}l^2c^{*2} + 2B^{12}hka^*b^* + 2B^{13}hla^*c^* + 2B^{23}klb^*c^*)].$$

	10 K	300 K	720 K
B^{11} [Pb]	1.04 (16)	2.15 (18)	4.92 (34)
B^{33} [Pb]	0.56 (20)	1.27 (24)	B^{11} [Pb]
B^{11} [Hf/Ti]	0.06 (61)	0.60 (46)	0.40 (51)
B^{33} [Hf/Ti]	−2.52 (95)	−2.71 (65)	B^{11} [Hf/Ti]
B^{11} [O1]	1.54 (37)	2.39 (40)	3.41 (98)
B^{33} [O1]	0.65 (32)	0.61 (30)	2.98 (64)
B^{11} [O2]	0.86 (32)	1.45 (34)	B^{11} [O1]
B^{22} [O2]	1.00 (32)	1.27 (30)	B^{33} [O1]
B^{33} [O2]	0.31 (24)	0.96 (26)	B^{11} [O1]

4. Splitting of the Hf/Ti crystallographic site

4.1. *Tetragonal structure*

In order to resolve the anomaly of the negative atomic displacement parameter along the c axis associated with the Hf/Ti pseudo-nucleus, a shift $\delta z_{cat} = z_{Hf} - z_{Ti}$ was introduced between these two cations. The z coordinates of the Hf and Ti nuclei were constrained so that their difference was δz_{cat}. Positive and negative values for δz_{cat} in the range −0.07 to +0.07 were tested in the refinement. Owing to high correlations between refined parameters (especially between the occupancy and the atomic displacement parameter), the occupancy x was fixed at 0.42, a value obtained in previous refinements above and below the Curie temperature and confirmed by EDS analysis.

The variation *versus* δz_{cat} of several parameters was studied using the refinement of the profiles collected at 10 and 300 K. Fig. 3(*a*), presenting the variation of the R_F factor at 300 K, exhibits two minima, at $\delta z_{cat} = -0.02$ and $\delta z_{cat} = +0.04$, the second corresponding to a better reliability factor. Moreover, the variation of the atomic z coordinates (Fig. 3*b*) shows that the physically acceptable solution is obtained for $\delta z_{cat} > 0$. With z_{O1} and z_{O2} remaining unchanged with δz_{cat}, the minimum observed for $\delta z_{cat} < 0$ corresponds to displacements in the opposite direction of Pb and Hf/Ti atoms with respect to the oxygen octahedron, contrary to that exhibited by $PbTiO_3$ (Glazer & Mabud, 1978) and $PbHfO_3$ (Madigou *et al.*, 1998). In Fig. 3(*c*), the B_{iso} [Hf/Ti] parameter is plotted at 300 K as a function of δz_{cat}: negative values are obtained for $|\delta z_{cat}| \leq 0.02$ and for $\delta z_{cat} = +0.04$ the atomic displacement parameter reaches a realistic value (B_{iso} = 0.63 Å^2) which compares well with the values obtained for Ti in $PbTiO_3$ [B_{iso} = 0.60 Å^2 (Shirane & Pepinsky, 1956)] at this temperature. Therefore, a shift $\delta z_{cat} = +0.04$ between Hf and Ti atoms improves the structure refinement and allows a physically reasonable

solution with a positive value for the B_{iso} [Hf/Ti] parameter.

Results of the tetragonal structure refinements performed with $\delta z_{cat} = z_{Hf} - z_{Ti} = +0.04$ are summarized in Table 4. Compared with the results obtained without splitting of the Hf/Ti positions, the z coordinates of the O1 and O2 atoms remain almost unchanged, but the Hf and Ti atoms are drastically displaced along the c axis, Ti moving farther than Hf with respect to the oxygen octahedron (Table 4). This is consistent with results previously obtained for $PbHfO_3$ and $PbTiO_3$. Indeed, the highest shift from the oxygen-octahedron centre of Hf atoms in $PbHfO_3$ {0.17 Å along the [100] direction of the orthorhombic cell (Madigou *et al.*, 1998)} is lower than that of Ti atoms in $PbTiO_3$ {0.32 Å along the [001] direction (Glazer & Mabud, 1978)}. This characteristic is also seen from the low spread of the interatomic distances Hf—O when compared with Ti—O (Table 5). Thus, there are strong clues that the Hf atom is closer to the centre of the oxygen octahedron than the Ti atom. Finally, the introduction of a splitting δz_{cat} in the refinement does not modify the value of δz_{Pb}, which is quite similar to that determined in $PbTiO_3$. Schematic projections on the (010) plane are displayed in Figs. 4(*a*) (10 K) and 4(*b*) (300 K).

Table 4. *Final results testing* $\delta z_{cat} = z_{Hf} - z_{Ti} = +0.04$ *in the Rietveld refinements*

	10 K	300 K	720 K
z_{Hf}	0.539 (3)	0.535 (2)	1/2
z_{Ti}	0.499 (3)	0.495 (4)	0.54 or 0.46 (fixed)
z_{O1}	0.095 (2)	0.079 (2)	0
z_{O2}	0.615 (2)	0.597 (1)	1/2
B_{iso} [Pb] (Å^2)	0.64 (11)	1.30 (11)	4.11 (28)
B_{iso} [Hf/Ti] (Å^2)	0.28 (26)	0.63 (22)	1.15 (40)
B_{iso} [O1] = B_{iso} [O2] (Å^2)	0.89 (8)	1.40 (7)	2.55 (12)
Hf occupancy (fixed)	0.42	0.42	0.42
R_{Bragg}	0.0671	0.0584	0.0278
R_F	0.0538	0.0508	0.0661
δz_{Pb} (Å)	0.446 (3)	0.373 (3)	0
δz_{Hf} (Å)	0.29 (1)	0.23 (1)	0
δz_{Ti} (Å)	0.45 (1)	0.39 (1)	0.16

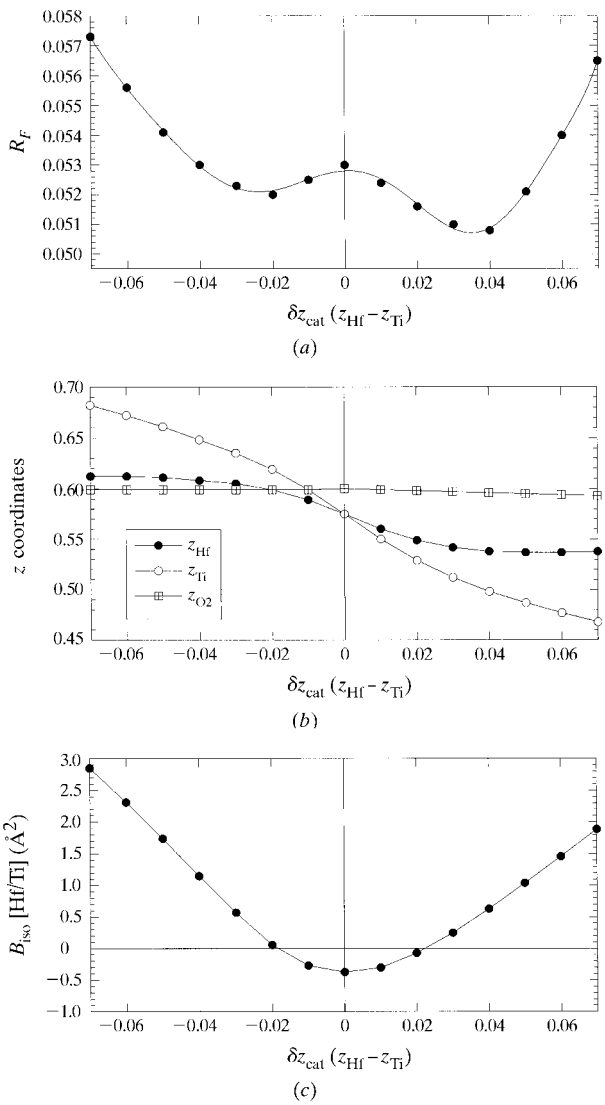

Fig. 3. Variation *versus* $\delta z_{cat} = z_{Hf} - z_{Ti}$ of (*a*) the R_F factor, (*b*) the atomic coordinates z_{Hf}, z_{Ti} and z_{O2}, and (*c*) the isotropic Hf/Ti atomic displacement parameter (data collected at 300 K).

The atomic displacement parameters associated with the O1, O2 and Pb atoms are similar to those obtained with $\delta z_{cat} = 0$. On the other hand, the B_{iso} [Hf/Ti] parameter reaches realistic positive values at 10 K as at 300 K (Table 4).

The calculated bond lengths in Table 5 confirm the statement in §3 about the distortion of the oxygen octahedra along the [001] direction. The O1*b* atom is much closer to the O2 plane than O1*a*. Thus, the greater displacement of the O1*a* atom can probably be correlated with z shifts of the Hf and Ti atoms in the same direction.

4.2. *Cubic structure*

For data collected at 720 K for the cubic phase, a shift $\delta z_{cat} = z_{Hf} - z_{Ti} = +0.04$ was also introduced in the structure refinement. Complete results are given in Table 4. As shown in Fig. 4(*c*), the titanium crystallographic site is split over six equivalent positions around the Hf atom placed on the centre of the oxygen octahedron. The shift between Hf and Ti is 0.16 Å (Table 4). The introduction of $\delta z_{cat} = +0.04$ in the refinement modifies the value of B_{iso} [Hf/Ti], which increases from 0.3 to 1.2 Å^2, the atomic displacement parameters of the Pb and O nuclei remaining unchanged when compared with the previous optimization without splitting. On the other hand, if the Ti atom is placed on the oxygen octahedron centre and the Hf atom is displaced from the idealized site (situation with $\delta z_{cat} <$ 0), the Hf/Ti displacement parameter becomes strongly

Table 5. *Bond lengths (Å) calculated from the models with* $\delta z_{cat} = z_{Hf} - z_{Ti} = +0.04$

	$PbTiO_3$, 300 K (Glazer & Mabud, 1978)	$PbHf_{0.4}Ti_{0.6}O_3$, 10 K	$PbHf_{0.4}Ti_{0.6}O_3$, 300 K	$PbHf_{0.4}Ti_{0.6}O_3$, 720 K
Hf—O1*a*	—	1.83 × 1	1.87 × 1	
Hf—O1*b*	—	2.29 × 1	2.23 × 1	2.02 × 6
Hf—O2	—	2.02 × 4	2.02 × 4	
Ti—O1*a*	1.77 × 1	1.66 × 1	1.71 × 1	1.86 × 1
Ti—O1*b*	2.39 × 1	2.46 × 1	2.39 × 1	2.18 × 1
Ti—O2	1.98 × 4	2.06 × 4	2.05 × 4	2.03 × 4
O2—O2	2.76 × 4	2.83 × 4	2.84 × 4	
O2—O1*a*	2.86 × 4	2.93 × 4	2.92 × 4	2.86 × 12
O2—O1*b*	2.84 × 4	2.81 × 4	2.82 × 4	
Pb—O1	2.80	2.85	2.86	
Pb—O2	2.52	2.55	2.60	2.86
Pb—O2	3.22	3.23	3.16	

negative (about -2.0 Å^2 for $\delta z_{cat} = -0.04$). Therefore, as has been shown previously, the physically reasonable solution is really obtained for $\delta z_{cat} > 0$. In conclusion, in the cubic phase one can consider the displacement of the titanium as a disordered shift with respect to the cubic symmetry, which takes a single direction below T_C in the ferroelectric tetragonal phase.

It is also noticeable that the B_{iso} [Pb] parameter is always higher than the others. The splitting of this atomic position from (0, 0, 0) to (x, x, 0) leads to a slightly improved refinement (the R_F factor decreasing from 0.0661 to 0.0640), with a final value $x = 0.05$ (17), which corresponds to a displacement of ~0.28 Å with reference to the unsplit position. In this way, the atomic displacement parameter drastically decreases from 4.1 to 1.8 Å^2, with other parameters remaining unchanged. Therefore, the high value of B_{iso} [Pb] seems to be correlated with a static or dynamic displacement of Pb around its ideal high-symmetry position. Displacement in the [110] direction gives good results probably because this direction is the most degenerate in cubic symmetry and thus describes well the anomalous high isotropic atomic displacement parameter associated with the Pb atom.

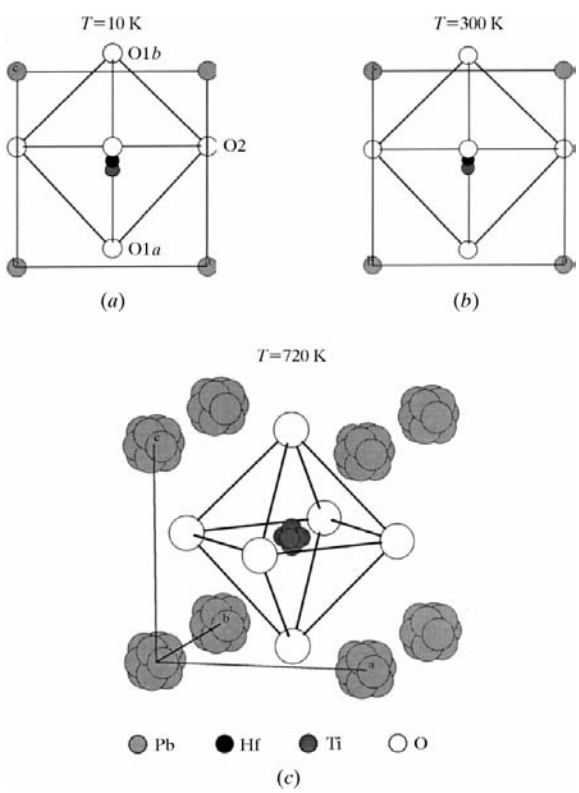

Fig. 4. Schematic projections on the (010) plane showing the relative displacement of the Hf, Ti and Pb nuclei in $PbHf_{0.4}Ti_{0.6}O_3$ at (*a*) 10 and (*b*) 300 K. A shift of $\delta z_{cat} = z_{Hf} - z_{Ti} = +0.04$ was introduced in the refinement. The conventional unit cell and oxygen octahedron are displayed. (*c*) A schematic view of the 720 K cubic structure: splittings of the Ti^{4+} and Pb^{2+} cation sites are drawn.

Describing the structure in a cubic symmetry implies that no electrical polarization exists. However, in the $PbHf_{0.4}Ti_{0.6}O_3$ paraelectric phase at 720 K a cooperative shift of Pb (0.28 Å) and Ti (0.16 Å) atoms relative to the oxygen network can be proposed leading to a local polarization in one unit cell. At long range (over a few unit cells) the cations statistically lie on disordered positions and so the average structure respects the cubic symmetry and the crystal is not polar.

5. Discussion

Through a peculiar behaviour of their mean-square atomic displacement parameter a shift between Hf and Ti atoms has been evidenced. In the tetragonal phase the high negative value of the B^{33} [Hf/Ti] parameter obtained from a conventional refinement is associated with a relative displacement of the Hf and Ti nuclei along z. A plausible explanation is related to the opposite values of the Hf and Ti nuclei coherent scattering lengths ($b_{Hf} > 0$, $b_{Ti} < 0$), leading to a phase shift of π in the structure factor. Taking into account an additional displacement δz_{cat} between the two cations the total phase shift between 0.42Hf and 0.58Ti is $\varphi = \pi + 2\pi.l.\delta z_{cat}$. As shown in Fig. 5 (representations drawn for $\delta z_{cat} = +0.04$ and $x = 0.42$), the relative phase shift, maximum for $\varphi = \pi$, decreases as the Miller index l

increases, *i.e.* the Hf/Ti pseudo-nucleus contribution to the structure factor increases along with the Bragg angle θ. This effect, opposite to that of the usual Debye–Waller factor, leads to a negative value of the calculated mean-square atomic displacement in a refinement not taking into account the atomic splitting.

In the high-temperature cubic phase, an additional phase shift to π between the hafnium and titanium contributions cannot be put forward to explain the very low value of the B_{iso} [Hf/Ti] parameter ($B_{iso} = 0.3$ Å^2), as the average positions of the Hf and Ti atoms are the same ($\frac{1}{2}, \frac{1}{2}, \frac{1}{2}$) from the cubic symmetry. However, the splitting of the Ti atom over six equivalent positions around ($\frac{1}{2}, \frac{1}{2}, \frac{1}{2}$) introduces a static B [Ti] factor, which reduces the contribution of Ti more and more as the Bragg angle increases. As $b_{0.42Hf} = 0.33 \times 10^{-12}$, $b_{0.58Ti} = -0.20 \times 10^{-12}$ cm and $|b_{0.42Hf}| > |b_{0.58Ti}|$, the resulting contribution $b_{Hf/Ti} = |b_{0.42Hf}| - |b^{red}_{0.58Ti}|$, where red indicates reduced, increases along with θ, which should again give a negative B [Hf/Ti] parameter in a refinement not taking into account the splitting. This effect is partly counterbalanced by the usual dynamic vibrational Debye–Waller factor with a final slightly positive global B [Hf/Ti] value.

Testing $\delta z_{cat} = +0.04$ in the refinement of the tetragonal and cubic phases, some parameters have been followed as a function of temperature. Fig. 6(*a*) shows the evolution *versus* temperature of the isotropic atomic displacement parameters for various ions. From $\delta z_{cat} = 0$ to $\delta z_{cat} = +0.04$ the curve describing the Hf/Ti vibrations is uniformly shifted and is quite parallel to that corresponding to the O atoms. Over the whole temperature range the value of B_{iso} [Pb] is significantly higher than B_{iso} [Hf] and similar to B_{iso} [O]. On the other hand, the evolution of B_{iso} [Pb] presents an anomaly above the Curie temperature, since it appears much larger than the others, which is unexpected for the heaviest atom in the structure. This anomaly can be removed when the idealized site of the Pb atom is split over 12 equivalent positions.

Finally, the thermal evolution of the z shifts with respect to the oxygen octahedron is presented in Fig. 6(*b*). It shows clearly that Pb displacement is as high as Ti. The introduction of δz_{cat} in the refinement of the cubic phase leads to a remanent Ti shift of ~0.16 Å above the Curie temperature.

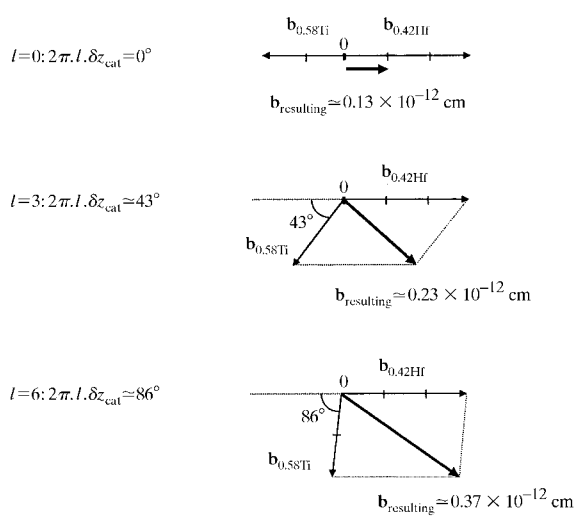

Fig. 5. Fresnel representations showing the evolution of the phase shift with l. Plots are displayed for $\delta z_{cat} = +0.04$ and $x = 0.42$.

6. Conclusions

From conventional refinements performed either for the ferroelectric tetragonal phase or for the paraelectric cubic phase some features of the mean-square atomic displacements of Pb and/or Hf/Ti nuclei have been evidenced. When a structural model of $PbTiO_3$ without atomic splitting is tested by refinement, the atomic displacement parameter associated with the Hf/Ti pseudo-nucleus becomes strongly negative in the low-temperature phase, especially along the [001] direction, and takes an unusual low positive value in the high-temperature phase. Below T_C, the introduction of a z shift $\delta z_{cat} = +0.04$ between Hf and Ti atoms leads to a positive value of the mean-square atomic displacements. Above T_C, in the cubic phase, the splitting of the Ti atom in a similar way over six equivalent positions around Hf

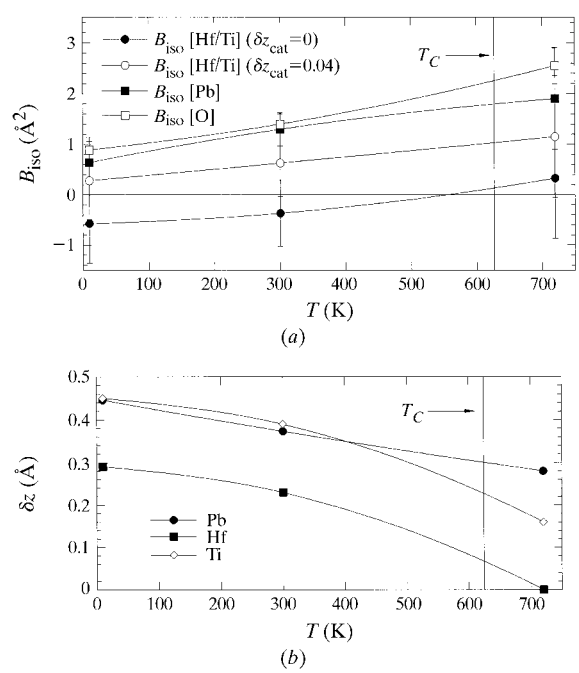

Fig. 6. Plot of (*a*) isotropic atomic displacement parameters and (*b*) z shifts *versus* temperature. In (*a*) plotted error bars are equal to three times the s.u.'s. The B_{iso} [Pb] parameter and the shift δz_{Pb} which are displayed are those obtained with the splitting of the Pb atom from its high-symmetry position (0, 0, 0) to the (x, x, 0) position.

resolves the anomaly. There is no doubt that the opposite values of the Hf and Ti coherent scattering lengths reinforce the signature of such atomic disorder and splitting, making them much easier to detect.

Moreover, in agreement with other studies performed on neighbouring compounds ($PbHfO_3$, $PbTiO_3$ and $PbSc_{1/2}Nb_{1/2}O_3$), a static or dynamic disorder on the Pb-atom sites has been proposed in the high-temperature cubic phase. When the Pb atom is displaced from the high-symmetry position (0, 0, 0) to one of the 12 equivalent (x, x, 0) positions, the atomic displacement parameter reaches a realistic value at the temperature considered.

References

Caglioti, G., Paoletti, A. & Ricci, F. P. (1958). *Nucl. Instrum.* **3**, 223–228.

Corker, D. L., Glazer, A. M., Dec, J., Roleder, K. & Whatmore, R. W. (1997). *Acta Cryst.* B**53**, 135–142.

Corker, D. L., Glazer, A. M., Kaminsky, W., Whatmore, R. W., Dec, J. & Roleder, K. (1998). *Acta Cryst.* B**54**, 18–28.

Favotto, C. (1997). PhD thesis, Université de Toulon et du Var, France.

Favotto, C., Margaillan, A. & Roubin, M. (1996). *Ann. Chim. Fr.* **21**, 13–24.

Favotto, C., Roubin, M., Idrissi, M. H. & Fantozzi, G. (1998). *J. Eur. Ceram. Soc.* In the press.

Floquet, N., Valot, C. M., Mesnier, M. T., Niepce, J. C., Normand, L., Thorel, A. & Kilaas, R. (1997). *J. Phys. III Fr.* **7**, 1105–1128.

Glazer, A. M. & Mabud, S. A. (1978). *Acta Cryst.* B**34**, 1065–1070.

Glazer, A. M., Mabud, S. A. & Clarke, R. (1978). *Acta Cryst.* B**34**, 1060–1065.

Glazer, A. M., Roleder, K. & Dec, J. (1993). *Acta Cryst.* B**49**, 846–852.

Jaffe, B., Roth, R. S. & Marzullo, S. (1955). *J. Res. Natl Bur. Stand.* **55**, 239–254.

Jankowska-Sumara, I., Kugel, G. E., Roleder, K. & Dec, J. (1995). *J. Phys. Condens. Matter*, **7**, 3957–3972.

Jona, F., Shirane, G., Mazzi, F. & Pepinsky, R. (1957). *Phys. Rev.* **105**, 849–856.

Kwapulinski, J., Pawelczyk, M. & Dec, J. (1994). *J. Phys. Condens. Matter*, **6**, 4655–4659.

Li, S., Huang, C.-H., Bhalla, A. S. & Cross, L. E. (1993). *Ferroelectr. Lett.* **16**, 7–19.

Madigou, V., Baudour, J.-L., Bouree, F., Favotto, C., Roubin, M. & Nihoul, G. (1998). *Philos. Mag. B.* In the press.

Malibert, C., Dkhil, B., Kiat, J.-M., Durand, D., Bérar, J.-F. & Spasojevic de Biré, A. (1997). *J. Phys. Condens. Matter*, **9**, 7485–7500.

Monceau, D. & Boudias, C. (1996). *CaRIne Crystallography*. Version 3.1. Divergent SA, Centre de Transfert, 60 200 Compiegne, France.

Nelmes, J., Piltz, R. O., Kuhs, W. F., Tun, Z. & Restori, R. (1990). *Ferroelectrics*, **108**, 165–170.

Rodriguez-Carvajal, J. (1990). *Fullprof. A Program for Rietveld Refinement and Pattern Matching Analysis*. Abstracts of the Satellite Meeting on Powder Diffraction of the XVth Congress of the International Union of Crystallography, p. 127.

Shirane, G. & Pepinsky, R. (1953). *Phys. Rev.* **91**, 812–815.

Shirane, G. & Pepinsky, R. (1956). *Acta Cryst.* **9**, 131–140.

Takeuchi, T., Ado, K., Saito, Y., Tabuchi, M., Masquelier, C. & Nakamura, O. (1995). *Solid State Ion.* **79**, 325–330.

Valot, C., Floquet, N., Mesnier, M. & Niepce, J.-C. (1996). *J. Phys. IV*, **3**, 71–89.